Temperature Effect on IgE Binding to CD23 Versus Fc εRI

Bing-Hung Chen, Michelle A. Kilmon, Check Ma, Timothy H. Caven, Yee Chan-Li, Anne E. Shelburne, Robert M. Tombes, Eric Roush and Daniel H. Conrad

This information is current as of March 20, 2012

References	This article **cites 38 articles**, 17 of which can be accessed free at: http://www.jimmunol.org/content/170/4/1839.full.html#ref-list-1
	Article cited in: **http://www.jimmunol.org/content/170/4/1839.full.html#related-urls**
Subscriptions	Information about subscribing to *The Journal of Immunology* is online at http://www.jimmunol.org/subscriptions
Permissions	Submit copyright permission requests at http://www.aai.org/ji/copyright.html
Email Alerts	Receive free email-alerts when new articles cite this article. Sign up at http://www.jimmunol.org/etoc/subscriptions.shtml/

Temperature Effect on IgE Binding to CD23 Versus FcεRI[1]

Bing-Hung Chen,* Michelle A. Kilmon,* Check Ma,* Timothy H. Caven,* Yee Chan-Li,* Anne E. Shelburne,* Robert M. Tombes,[†] Eric Roush,[‡+] and Daniel H. Conrad[2]*

A chimeric soluble CD23, consisting of the extracellular domain of mouse CD23 and a modified leucine zipper (*lz*-CD23), has been shown to inhibit IgE binding to the FcεRI. A similar human CD23 construct was also shown to inhibit binding of human IgE to human FcεRI. In both systems, the inhibition was found to be temperature dependent; a 10-fold molar excess of *lz*-CD23 gave 90–98% inhibition at 4°C, dropping to 20–30% inhibition at 37°C. Surface plasmon resonance analysis of lz-CD23 binding to an IgE-coated sensor chip suggested that the effective concentration of lz-CD23 was lower at the higher temperatures. Analysis of ^{125}I-IgE binding to CD23$^+$-Chinese hamster ovary cells also indicated that increased temperature resulted in a lower percentage of IgE capable of interacting with CD23. In contrast, IgE interacts more effectively with FcεRI$^+$-rat basophilic leukemia cells at 37°C compared with 4°C. The results support the concept that the open and closed IgE structures found by crystallography interact differently with the two IgE receptors and suggest that temperature influences the relative percentage of IgE in the respective structural forms. Changes in CD23 oligomerization also plays a role in the decreased binding seen at physiological temperatures. *The Journal of Immunology,* 2003, 170: 1839–1845.

The FcεRI is one of the best characterized of the FcR. Discovered initially on mast cells and basophils where crosslinking results in allergic mediator release, it is now known to be on a variety of hemopoietic cells, at least in humans (reviewed in Ref. 1). When expressed on mast cells and basophils, it consists of three different subunits with the stoichiometry of $\alpha\beta\gamma_2$ while expression on other cell types is $\alpha\gamma_2$ (2, 3). The low-affinity receptor for IgE (FcεRII/CD23), discovered initially on lymphocytes, consists of a single polypeptide chain (reviewed in Ref. 4). A variety of experiments have indicated that CD23 is a homotrimer while at the cell surface (5, 6). Cleavage by metalloprotease(s) results in the release of the IgE-binding lectin domain and dissociation of the trimer (7). CD23 is known to enhance Ag processing of IgE-Ag complexes (8) and, more recently, it has been implicated, primarily through the use of CD23 KO and transgenic mice, in regulation of IgE synthesis (9, 10).

Data using peptides derived from the Fc region of IgE as well as mAbs directed against the Fc region of IgE indicated that the two IgE receptors interact with closely adjacent, but not identical, sites on the Fc region of IgE (11, 12). Recent analysis of IgE-Fc/FcεRIα crystals have confirmed that the interaction site for the FcεRI is in the Cε3 domain of IgE (13). Although crystal information is not currently available for the CD23-IgE interaction, the Cε3 domain is implicated by the studies mentioned above. Further confirmation of the closeness of the sites is seen in the capacity of a soluble trimeric CD23 chimera to block binding of IgE to the FcεRI in both the mouse and human systems (14, 15). This chimera consists of an isoleucine zipper motif linked to the N terminus of the extracellular region (aa 48–331) of CD23 (*lz*-CD23$^{48-331}$) (15). The studies reported here were initiated to investigate the capacity of lz-CD23 to inhibit mediator release from mast cells. The finding that, depending on the temperature of sensitization, little inhibition of mediator release was seen led us to examine the effect of temperature on the binding of IgE to both the FcεRI and CD23. IgE was found to interact more efficiently with CD23 at lower temperatures (4–20°C) while the inverse was seen with the FcεRI, namely, more efficient interaction with IgE occurred at 37°C. Reasons for this difference are potentially the "open" and "closed" isoforms seen in the crystal structure of IgE Fc (16) as well as increased instability of the CD23 trimer at the higher temperatures.

Materials and Methods

Cell lines, media, and reagents

The preparation of both the murine and human chimeric *lz*-CD23 that was used in this study is described elsewhere (14) and are *lz*-CD23$^{86-331}$ and *lz*-CD23$^{139-331}$. The rat basophilic leukemia (RBL-2H3) cell line (a gift from Dr. J. Rivera, National Institute of Arthritis and Musculoskeletal and Skin Diseases, National Institutes of Health, Bethesda, MD) was maintained in MEM supplemented with 10 mM HEPES (pH 7.4), 16.7% FBS, 100 U/ml penicillin and streptomycin, and 2 mM glutamine. RBL-2H3 transfected with the human FcεRIα chain (17) was a gift from Dr. J.-P. Kinet (Harvard Medical School, Boston, MA). CD23 expressing Chinese hamster ovary K1 cells, Fc1.7, were made as previously described (5) and grown in DMEM containing glutamate. Rat IgE (IR162) (18) and monoclonal mouse IgE (mIgE^3-DNP) (19) from H1-DNP-ε-26 were purified from ascites as described previously (20). Human myeloma IgE (PS) was a gift from Dr. K. Ishizaka (Pharmaceutical Research Laboratory, Kirin Brewery Company, Gunma, Japan) and recombinant human IgE Fc (a gift from Dr. A. Beavil (Kings College, London, U.K.)) was prepared as described elsewhere (21). Mouse and rat IgE were labeled with [^{125}I]NaI (NEN Life Science, Boston, MA) using the chloramine-T method as previously described (22). DNP-BSA and *p*-nitrophenyl-*N*-acetyl-β-D-glucosaminide were purchased from Calbiochem-Novabiochem (La Jolla, CA) and Sigma-Aldrich (St. Louis, MO), respectively.

Departments of *Microbiology and Immunology and [†]Biology, Virginia Commonwealth University, Richmond, VA 23298; and [‡]Biacore, Inc., Piscataway, NJ 08854

[2] Address correspondence and reprint requests to Dr. Daniel H. Conrad, Department of Microbiology and Immunology, Virginia Commonwealth University, Box 980678, MCV Station, Richmond, VA 23298-0678. E-mail address: dconrad@hsc.vcu.edu

[3] Abbreviations used in this paper: mIgE, mouse IgE; SPR, surface plasmon resonance; RU, resonance units; FRET, fluorescent resonance energy transfer; EDC, 1-ethyl-3-(3-dimethylaminopropyl)carbodiimide hydrochloride; CFP, cyan fluorescent protein; YFP, yellow fluorescent protein; sCD23, soluble CD23.

Sensitization of RBL-2H3 Cells and β-hexosaminidase release assay

On the day of the experiment, RBL-2H3 cells (5×10^6 cells/ml) were resuspended in medium containing 10 mM HEPES (pH 7.4) and 2 mM CaCl$_2$ before mixing with an equal volume of either mIgE-DNP (200 ng/ml) alone or the reaction mixture containing the same concentration of mIgE-DNP plus *lz*-CD23. After incubation at the indicated temperatures (range, 4–37°C) for 1.5 h, cells were washed once with HBS/Ca^{2+} (0.01 M HEPES buffered saline containing 2 mM CaCl$_2$) and twice with Tyrode's buffer (135 mM NaCl, 5 mM KCl, 1 mM MgCl$_2$, 1.8 mM CaCl$_2$, 5.6 mM glucose, and 20 mM HEPES (pH 7.4)) containing 0.05% BSA to remove unbound IgE. Cells were then incubated with Tyrode's/0.05% BSA buffer containing DNP-BSA at different concentrations (0, 0.01, 0.1, 1, 10, 100, and 1000 ng/ml) for 1 h at 37°C before an aliquot of supernatant was removed for β-hexosaminidase analysis. Supernatants taken from cells without DNP-BSA added or cells lysed by detergent (cold Tyrode's buffer with 0.5% Triton X-100) were also analyzed to measure the spontaneous and complete release of β-hexosaminidase, respectively, using a previously published protocol (23). After subtraction of spontaneously released enzyme, inhibition of β-hexosaminidase secretion was expressed as a percentage of the enzyme release occurring in the absence of any *lz*-CD23 proteins.

^{125}I-IgE binding analysis

Increasing amounts of chimeric CD23 proteins were added to constant amounts of ^{125}I-mIgE or human IgE and the reactions were kept at the indicated temperatures (range, 4–37°C) for 30 min. This was then followed by the addition of 1×10^6 FcεRI$^+$ RBL-2H3 cells (with human IgE, RBL transfected with human FcεRIα were used), and the incubation was kept at the same temperature as the previous step for an additional 60 min. At the end of the incubation, a phthalate oil cushion centrifugation procedure (24) was used to separate free from cell-bound ^{125}I-IgE. The cell-bound radioactivity of each reaction was determined in duplicate on an LKB-Wallac CliniGamma-1272 automatic gamma counter. Specific binding of samples was calculated by subtracting background controls incubated with 100-fold excess of cold mIgE and compared with controls without any inhibitor added. Percent inhibition was calculated as follows: $(1 -$ (cpm experimental $-$ cpm 100-fold excess of unlabeled IgE)/(cpm control with no inhibitor $-$ cpm 100-fold excess of unlabeled IgE)$) \times 100$. Bindability of IgE was determined by incubating ^{125}I-mIgE (50 ng/ml) with excess cells, ranging from 2.0×10^6 to 2.5×10^7 Fc1.7 or RBL-2H3 cells in a volume of 1 ml. After a 60-min incubation, the cells were spun down and the amount of unbound ^{125}I-mIgE in the supernatant was counted to determine the amount of unbound IgE. The fraction of bound IgE was calculated as follows: $1 -$ (cpm unbound IgE/cpm of total IgE added). Using the linear extrapolation method published by Lindmo et al. (25), the binding data were plotted as a double inverse plot. The inverse of the intercept value represents the fraction of bindable IgE. The equilibrium of IgE binding to FcεRI was determined by incubating 5×10^5 RBL-2H3 cells with 25 ng ^{125}I-mIgE for the indicated amount of time. A fraction of the cells was spun over phlatate oil (26) to determine the amount of IgE bound. The cpm bound was adjusted for nonspecific binding by subtracting the cpm of cells incubated with a 100-fold excess cold mIgE.

Scatchard analysis

The affinity of IgE for CD23 was determined as previously described (5). Briefly, 5×10^5 Fc1.7 cells were added to tubes and allowed to equilibrate to the appropriate temperature. ^{125}I-labeled IgE (0.5 or 5.0 μg) was added to the cells along with increasing amounts of cold IgE, resulting in a final concentration range of 1.0 to 400 μg/ml. The tubes were incubated for 60 min on ice and the free and cell-bound ^{125}I-IgE was separated on a phthalate oil mixture as described above. Nonspecific binding was determined by adding 100-fold excess cold IgE and the value was subtracted to obtain specific binding. Binding affinities were determined by linear regression analysis.

Surface plasmon resonance (SPR) analysis

The Biacore X or the Biacore 3000 (Biacore, Uppsala, Sweden) was used to perform SPR measurements. Either rat or human IgE (1000–1500 resonance units (RU)) were coupled directly to the CM5 chip using the aminecoupling kit. All binding experiments used HBS/Ca^{2+} (0.01 M HEPES buffered saline containing 2 mM CaCl$_2$) as the running buffer and a flow rate of 20 μl/min. Different concentrations of lz-CD23 were passed over the control (no protein immobilized) and test flow cells by the use of the multichannel flow option. HBS buffer containing 20 mM EDTA (pH 8.0) was used between injections to elute bound recombinant CD23. The BI-

AEVALUATION 3.2 software (Biacore) was used for the analysis of interaction kinetics. The best fit for the data was obtained using a previously published model (14, 27) where the analyte (*lz*-CD23) interacts with two independent sites on the immobilized ligand (*A* plus *B1* plus *B2* = *AB1* plus *AB2*). In this analysis, the *A* parameter is *lz*-CD23 and *B1* and *B2* represent the two different binding sites on IgE. The decrease in available IgE was compared by injecting the same *lz*-CD23 concentration over the chip after equilibration at each respective temperature. The maximum RU obtained were determined and plotted vs the temperature of the assay.

Chemical cross-linking and fluorescent resonance energy transfer (FRET)

The chemical cross-linking protocol was as published previously(14), using the reagent 1-ethyl-3-(3-dimethylaminopropyl)carbodiimide hydrochloride (EDC; Pierce, Rockford, IL.). Cross-linking times were 1 h at 37°C and 2 h at 4°C. Subsequently, 1 μg of cross-linked or control (no EDC) lz-CD23 was analyzed by SDS-PAGE, followed by Western blot analysis using a polyclonal anti-CD23 followed by goat anti-rabbit IgG-HRP for detection (14). Bands were visualized using ECL substrate (Pierce) and the Alpha Innotech Fluro-Chem 8800 imaging system (Alpha Innotech, San Leandro, CA).

The lz-CD23 was transferred into pECFP-C1 and pEYFP-C1 (both from Clontech Laboratories, Palo Alto, CA) by PCR using primers that added a 5′ *Sal*I site (GTCGACATGAAACAGATAGAGGATAAGATCG) and a 3′ *Hpa*I site (GTTAACCTTTCAGCAAAAAACCCCTCAAGAC). This produced *lz*-CD23$^{86-331}$ with either enhanced cyan fluorescent protein (CFP) or enhanced yellow fluorescent protein (YFP) in frame at the amino terminus, depending on the vector (*lz*-CD23-pECFP-C1 and *lz*-CD23-pEYFP-C1). As a control, the entire CD23 cDNA was transferred into pECFP-C1 and pEYFP-C1 by PCR again using a 5′ *Sal*I site (GTCGACG GATCCATGGAAGAAAATGAATACTCAGG) and a 3′ *Hpa*I site (GT TAACTCTTCTGAGATGAGTTTTTGTTCGAAGGG). This produced CD23 with either a CFP or YFP in frame at the amino terminus, depending on the vector (CD23-pECFP-C1 and CD23-pEYFP-C1). Control vectors containing Fas-CFP and Fas-YFP (28) were gifts from Dr. M. J. Lenardo (National Institutes of Health, Bethesda, MD). The CFP and YFP fusion proteins were, singly or in combination, transfected into 3×10^5 293T cells using Fugene 6 (Roche Diagnostics, Indianapolis, IN) according to the manufacturer's instructions. After 2 days, cells were collected by centrifugation, resuspended in 200 μl of HBBS/1% FBS and placed into a black-sided 96-well plate (3603; Corning Glass, Corning, NY). A PerkinElmer Victor2 fluorometer (PerkinElmer, Norwalk, CT) was used to measure FRET. CFP is measured at 430/10 excitation and 490/40 emission. YFP is measured at 485/14 excitation and 535/30 emission. FRET is measured at 430/10 excitation and 535/30 emission. Fluorescence was background subtracted and FRET values were calculated using equation 11 from Ref. 29, which corrects for fluorochrome concentration and spectral overlap. Spectral overlap of YFP alone was ~4% and CFP alone was ~17%, which was comparable with published values (29, 30).

Results

Inhibition of mediator release by lz-CD23

Based on our initial studies indicating that *lz*-CD23 had the capacity to block binding of IgE to the FcεRI, we wished to determine whether mediator release was also effectively inhibited. Initial studies were performed by sensitizing the RBL cells at 37°C in the presence of *lz*-CD23 and minimal inhibition of mediator release was seen (data not shown). This was further investigated by performing the sensitization step at various temperatures. As seen in Fig. 1*A*, the effectiveness of mediator release inhibition was inversely proportional to temperature. The *inset* of Fig. 1*A* shows a plot of effectiveness of mediator release inhibition as a function of temperature using additional temperature points. As previously indicated (14) *lz*-CD23$^{139-331}$ is the minimum-sized chimera retaining IgE-binding activity and at 4°C this was equally effective in inhibiting IgE binding as the initially prepared *lz*-CD23$^{48-331}$ chimera (15). To determine whether the full-size *lz*-CD23 would be more stable at elevated temperature, we determined the capacity of *lz*-CD23$^{86-331}$ (which contains the complete coiled-coil stalk region) to both inhibit IgE binding to RBL cells as well as block β-hexaminidase release. As is seen in Fig. 1*B*, this chimera is
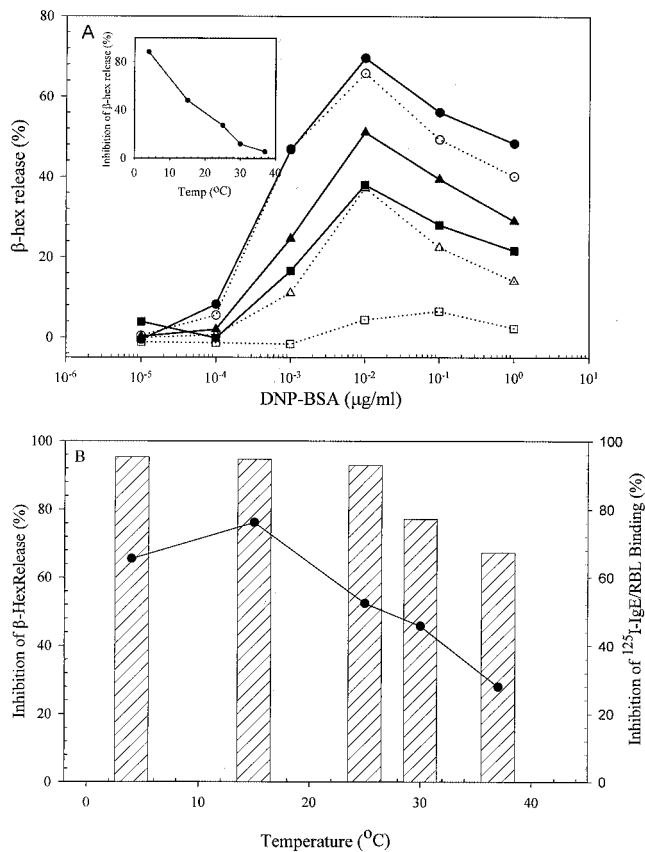
FIGURE 1. The inhibitory capacity of lz-CD23$^{139-331}$ on β-hexosaminidase release from sensitized RBL-2H3 cells is temperature dependent. A, mIgE-anti-DNP (200 ng) was incubated, either alone ($\bullet$, $\blacktriangle$, and $\blacksquare$) or along with 200-fold excess of lz-CD23$^{139-331}$ ($\bigcirc$, $\triangle$, and $\square$) at the indicated temperatures ($\bullet$,$\bigcirc$, 37°C; $\blacktriangle$,$\triangle$, 25°C; $\blacksquare$,$\square$, 4°C) for 30 min. RBL-2H3 were then added and incubation was continued at the indicated temperature for 1 h. Cells were then washed and incubated with indicated levels of DNP-BSA for 1 h. Supernatant aliquots were analyzed for β-hexosaminidase (β-hex) release. $Inset$ shows percentage of β-hexosaminidase release by lz-CD23$^{139-331}$ at the maximum release point (10^{-2} μg/ml DNP-BSA) plotted against temperature. B, Temperature dependence of inhibition for β-hexosaminidase release ($\bullet$) or ^{125}I-IgE binding ($\boxed{\diagup}$), respectively, using lz-CD23$^{86-331}$.

FIGURE 2. Dose dependence of lz-CD23-mediated inhibition of IgE binding at different temperatures. Mouse lz-CD23$^{139-331}$ (A) or lz-huCD23$^{45-321}$ (B) were incubated with 100 ng of ^{125}I-labeled mouse or human IgE, respectively, at the temperatures indicated. After 30 min, RBL-2H3 (A) or RBL-2H3 expressing human FcϵRI (17) (B) were added after another 1-h incubation, cell-bound radioactivity was determined, and the inhibitory effect was determined. See $Materials$ and $Methods$ for additional details.

somewhat less influenced by temperature; however, a clear decrease in both inhibitory capacities is seen as temperatures are increased. The decrease in effectiveness of mediator release inhibition as compared with IgE binding is noted; an explanation for this would be that a relatively small amount of bound Ag-specific IgE is sufficient to give normal mediator release values. Based on these results, the temperature effect on IgE binding was examined in the human systems. Fig. 2 shows the inhibitory capacity of increasing doses of mouse or human lz-CD23 to block binding of their respective ^{125}I-IgE. As can be seen, while very effective inhibition of IgE binding to the FcϵRI occurs at 4°C, this inhibitory capacity dropped to ~30–50% maximum at 37°C in both human and mouse systems.

SPR analysis of lz-CD23-IgE interaction at various temperatures

The temperature effect could either be a result of a change in IgE or in either of the IgE receptors, respectively. To investigate this issue, IgE was coupled to a CM5 sensor chip and SPR analysis was performed at different temperatures. Fig. 3 shows an experiment where different doses of mouse lz-CD23$^{139-331}$ were passed over
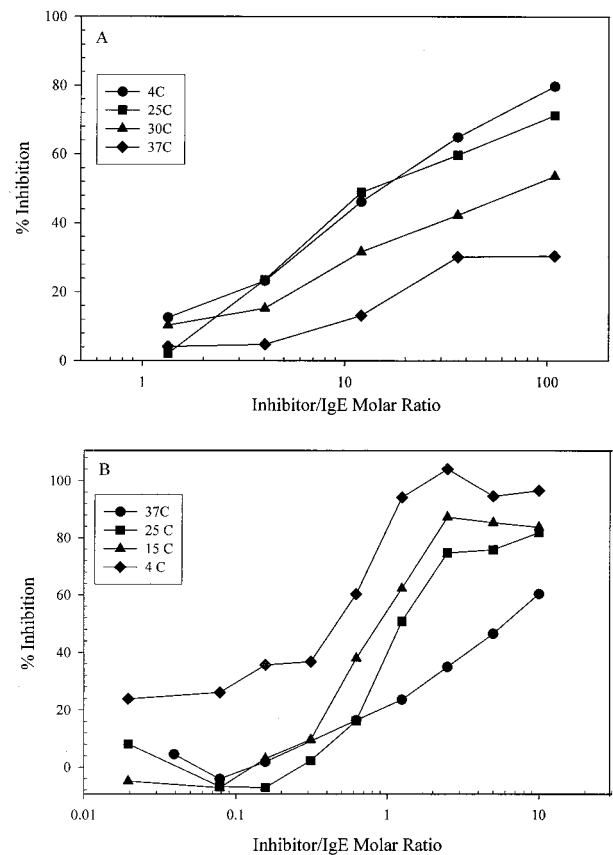
a rat IgE sensor chip at either 15°C (Fig. 3A) or 35°C (Fig. 3B), respectively, and Table I shows the kinetic parameters calculated for this interaction. As indicated by Chen et al. (14), the best fit for the data was obtained using a two-site model system. Note that the changes in the kinetic binding parameters is relatively small, indicating that with respect to SPR analysis, the IgE detected is binding with a similar affinity (see $Discussion$). However, a consistent finding is that the binding plateaus at a decreasing level, depending on the temperature. Very similar results were seen when human IgE and human lz-CD23 were used instead of the rodent reagents. This finding is illustrated in Fig. 4 which is a graphical representation of the maximum RU signal obtained with the same concentration of lz-CD23 used at the temperatures indicated. The decrease is seen somewhat earlier for human IgE-human lz-CD23, but in both systems a similar decrease in "available" IgE is seen. Note that the change is reversible in that after the 40°C step, returning the temperature to 8°C restored the binding level (data not shown). In separate experiments, 95 and 94% of the maximum binding were seen when either the mouse or human lz-CD23 were returned to 15°C subsequent to the higher temperature study (data not shown). These results indicate that IgE becomes increasingly inaccessible to lz-CD23 as the temperature of the interaction is increased; however, the proportion of IgE still accessible interacts with similar kinetic parameters; indeed, if any change, the affinity is slightly increased at elevated temperatures.
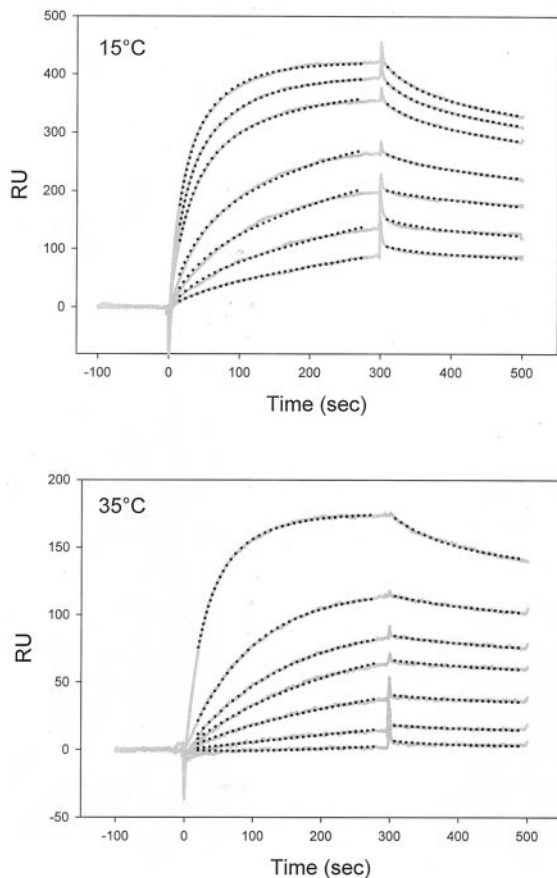
FIGURE 4. Plateau binding of *lz*-CD23 binding decreases with temperature. A sensogram for the interaction of rat IgE (●) or human IgE (○) CM5-coupled sensor chip was run at a constant concentration (800 nM) of either mouse *lz*-CD23[86–331] or human *lz*-CD23[45–321], respectively. The graph shows the plateau RU value for either preparation vs temperature.

FIGURE 3. SPR analysis of *lz*-CD23[139–331] binding to rat IgE at different temperatures. A CM5 sensor chip coated with 1000 RU of rat IgE was used to analyze the binding parameters of *lz*-CD23[139–331] at 15°C (*A*) vs 35°C (*B*). Different concentrations (800, 600, 400, 200, 100, 50, and 25 nM, respectively) of *lz*-CD23[139–331] were injected at a volume of 100 μl, with a delay time of 200 s, through the sensor chip surface. Bound *lz*-CD23 was removed with HBBS buffer containing 20 mM EDTA in between injections (see *Materials and Methods*).

Temperature influence of binding of IgE to cell surface CD23 or FcεRI

To confirm the temperature dependence of the binding seen above, binding studies with cells expressing either CD23 or the FcεRI were used. One way of determining the maximum binding ability of IgE is to add increasing concentrations of receptor-bearing cells to a fixed concentration of IgE. Using the method published by Lindmo et al., (25), the maximum bindability can be determined by appropriate extrapolation. Fig. 5*A* shows the bindability of IgE to CD23 at 4 and 37°C, respectively, and the *inset* of this figure shows the double reciprocal plot extrapolated to show bindability. As can be seen, the bindability of IgE at 37°C is ~50% of the value found at 4°C. Scatchard analysis of IgE binding to CD23 shows that the number of binding sites at both temperatures is
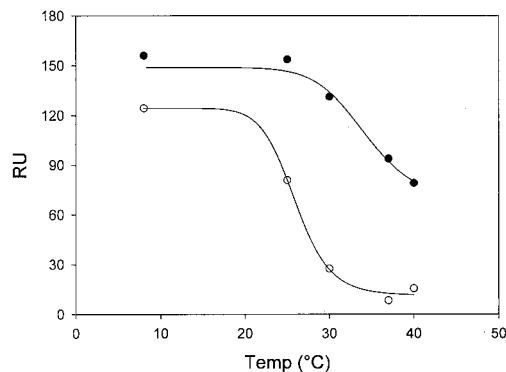
similar; however, the affinity of IgE for CD23 appears to be lower at the higher temperature (Fig. 5*B*). Fig. 6*A* shows a similar experiment performed with FcεRI using RBL cells. The inverse is seen in that binding is more efficacious at 37°C with the FcεRI. The slow k_1 reported for the FcεRI at 4°C precludes Scatchard analysis, since equilibrium is not achieved in this time frame, but the binding is clearly much more effective at 37°C as compared with 4°C for binding to the FcεRI. This issue is further addressed in Fig. 6*B*, where binding to the FcεRI is shown as a function of time. Given sufficient time, the plateau level of binding seen at 37°C is achieved at the lower temperature.

lz-CD23 remains associated at 37°C

The trimeric configuration of *lz*-CD23 results in an increased capacity to bind IgE due to the avidity resulting from two lectin domains interacting with the IgE Fc (31). In contrast, monomeric soluble CD23 (sCD23) interacts only weakly with IgE due to the loss of this avidity effect (32). To determine whether *lz*-CD23 dissociated as a function of temperature, thus explaining the loss of FcεRI-inhibiting activity, *lz*-CD23 was subjected to chemical cross-linking and FRET analysis. As shown in Fig. 7*A*, effective cross-linking with EDC was observed for both *lz*-CD23[86–331] (*lane 1* vs *lane 2*) and *lz*-CD23[139–331] (*lane 3* vs *4*) which show EDC cross-linked vs uncross-linked, respectively. The data shown are from cross-linking performed at 37°C; cross-linking at 4°C gave similar results (data not shown). The molecular mass of the cross-linked band, determined using the molecular mass markers, was 104,200 and 86,600 daltons for *lz*-CD23[86–331] and *lz*-CD23[139–331], respectively; which corresponds to the trimer molecular mass. Note that some dimer is evident in the uncross-linked *lz*-CD23 (*lanes 2* and *4*), indicating that the molecular association is resistant to complete dissociation, even with SDS.

In addition, the green fluorescent protein analogs, CFP and YFP, which are a donor-acceptor pair for FRET, were attached in frame

Table I. *Kinetic parameters*[a]

Temperature (°C)	k_{a1}	k_{a2}	k_{d1}	k_{d2}	K_{A1}	K_{A2}
15	4.98×10^4	2.05×10^4	2.09×10^{-2}	5.69×10^{-4}	2.38×10^6	3.60×10^7
25	3.10×10^4	2.48×10^4	2.08×10^{-2}	4.21×10^{-4}	1.49×10^6	5.89×10^7
35	3.94×10^4	1.81×10^4	1.04×10^{-2}	1.91×10^{-4}	3.79×10^6	9.48×10^7

[a] Values (k_a s^{-1}M^{-1} and k_d s^{-1}) were determined from SPR analyses using the cooperative model described elsewhere (14). The two K_A (M^{-1}) values are k_{a1}/k_{d1} and k_{a2}/k_{d2}, respectively. The values are determined using the concentrations shown in Fig 3.
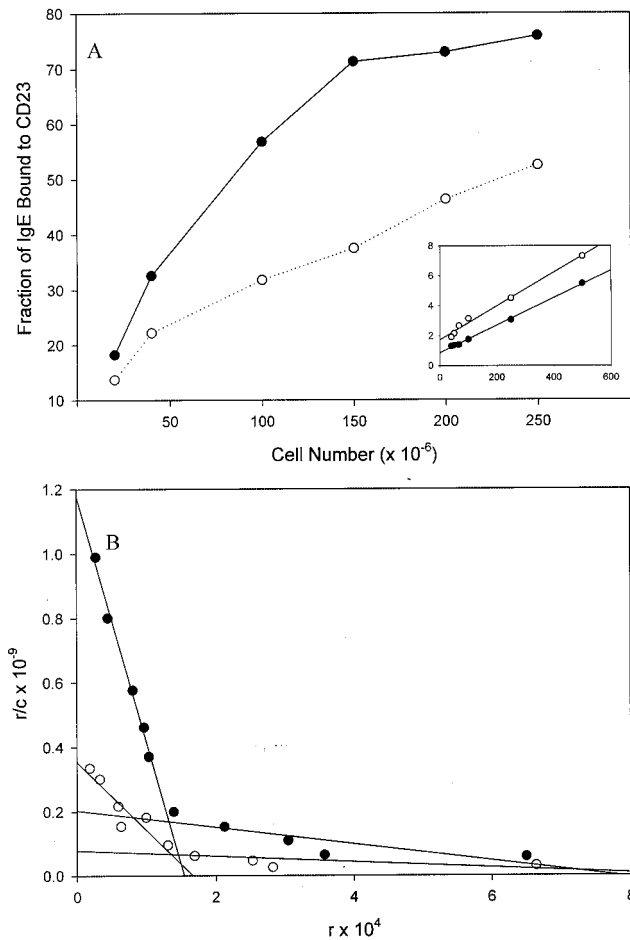
FIGURE 5. IgE binding to membrane CD23 is temperature dependent. *A,* The percentage of IgE bindable to CD23 at both 4°C (●) and 37°C (○) was determined. ^{125}I-IgE was incubated with the indicated number of excess Fc1.7 cells at the respective temperature and the percent bound was calculated as described in *Materials and Methods*. The *inset* represents the binding data plotted as a double inverse plot using linear regression. The inverse of the intercept represents the amount of bindable IgE. *B,* Scatchard analysis was performed to determine the affinity of IgE for CD23 at different temperatures. Fc1.7 cells were incubated with increasing concentrations of ^{125}I-IgE at either 4°C (●) or 37°C (○). After 1 h, cell-bound cpm was determined on duplicate aliquots of cells. The lines represent regression analysis.
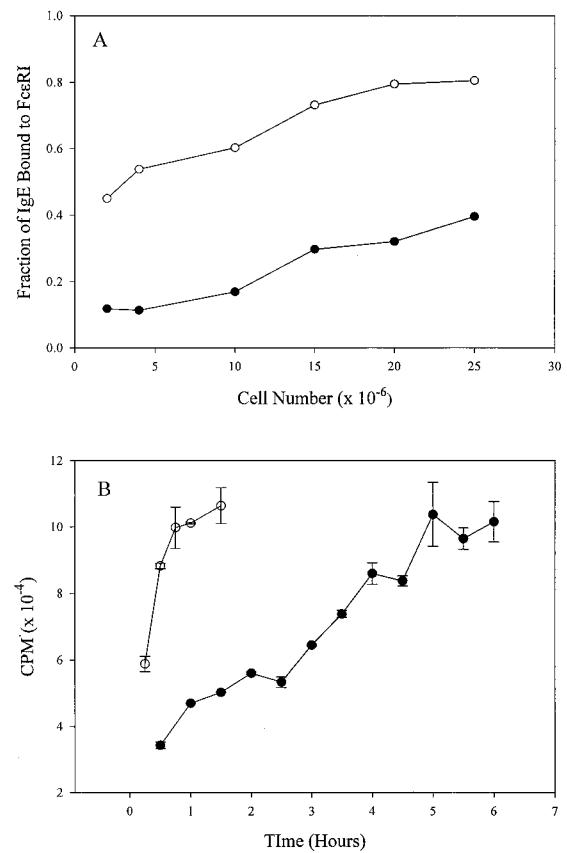

FIGURE 6. IgE binding to FcεRI is also temperature dependent. *A,* The percentage of IgE bindable to FcεRI at 4°C (●) and 37°C (○) was determined using RBL-23H cells. *B,* The kinetics of IgE binding to FcεRI at both temperatures was determined. RBL-2H3 cells were incubated with ^{125}I-IgE at 4°C (○) or 37°C (●) for the length of time specified and the amount of IgE bound was determined.

to the amino terminus of *lz*-CD23$^{86-331}$. Cells transiently transfected with *lz*-CD23-CFP and *lz*-CD23-YFP were analyzed for FRET signal as described in *Materials and Methods*. As is seen in Fig. 7*B*, an excellent FRET signal was seen for *lz*-CD23 and indeed the signal intensity, which was corrected for fluorophore concentration (29), was up to an order of magnitude better for *lz*-CD23 than membrane CD23 (see *Discussion*). Importantly, the FRET signal was not significantly influenced by temperature, further demonstrating that *lz*-CD23 does not dissociate at the higher temperatures. As a positive control, Fas-CFP/YFP transfection is shown and as reported previously (28), a good FRET signal is seen. CD23-CFP and Fas-YFP were cotransfected as a negative control and the calculated FRET signals were negative; they are shown as zero in Fig. 7*B*.

Discussion

With the cloning of CD23 and the FcεRI, the different origin and nature of the two IgE receptors became obvious. As mentioned in

the introduction, however, a substantial amount of data indicated that the site(s) on the Fc region of IgE in the Cε3 domain where the two receptors interact, while not identical, were quite close. This suggested that a soluble version of CD23 could act as an inhibitor of IgE binding to the FcεRI. The naturally produced sCD23 interacts with IgE with a low affinity, making such a strategy implausible. However, a chimeric sCD23, in which an isoleucine zipper motif was linked to the amino-terminal end of the extracellular domain of CD23, was recently shown to both bind IgE at least as effectively as membrane-expressed CD23 (15). The rationale for this increased binding was that the isoleucine zipper motif stabilized the coiled-coil stalk region of the soluble molecule in much the same manner as the transmembrane/cytoplasmic region does with the cell-expressed molecule. Although the exact stoichiometry of the *lz*-CD23 oligomer has not been elucidated, cross-linking data (14) indicate that trimeric and dimeric complexes are favored. Such structures allow a multivalent interaction with two sites on the IgE Fc and molecular modeling (33) combined with thermodynamic studies indicate that the two sites are not identical (31). These biochemical studies led the current model for membrane and *lz*-CD23 structure, namely, a trimer of either the naturally expressed membrane molecule or the engineered *lz*-CD23 (15, 33).

The development of a sCD23 that interacted effectively with IgE made it possible to reinvestigate the capacity of CD23 to block binding to the FcεRI and, indeed, in both the mouse (15) and human (14) systems an effective inhibition of binding was seen.
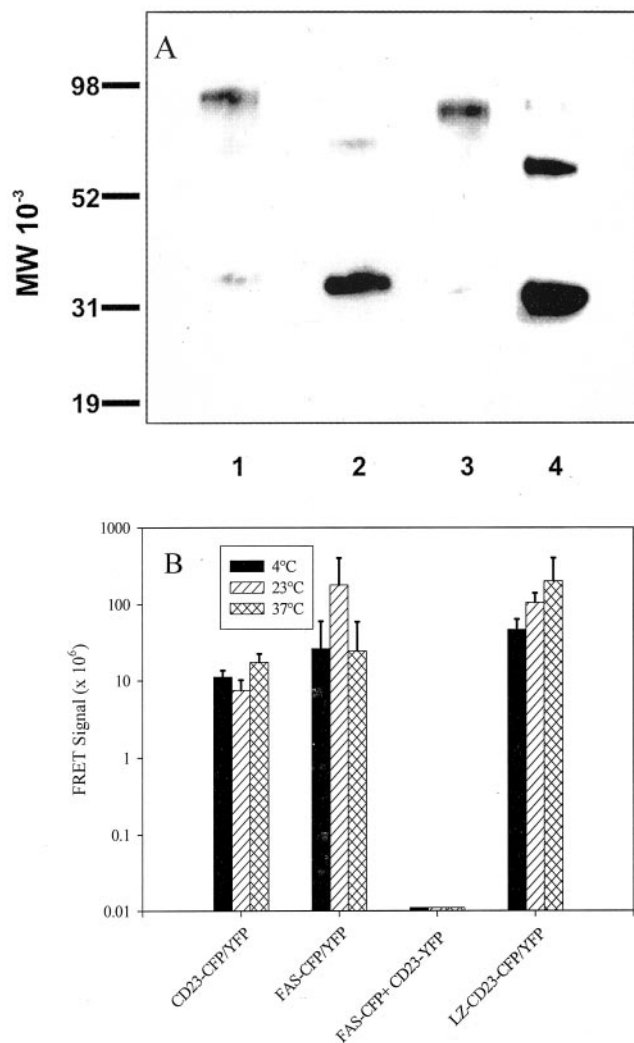
FIGURE 7. *lz*-CD23 remains associated at 37°C. To demonstrate that *lz*-CD23 remains associated at the temperatures used in this study, *lz*-CD23 was subjected to chemical cross-linking (*A*) or FRET analysis (*B*). *A, lz*-CD23$^{86-331}$ (*lanes 1* and *2*) or *lz*-CD23$^{139-331}$ (*lanes 3* and *4*) was either EDC cross-linked (*lanes 1* and *3*) or buffer treated (*lanes 2* and *4*) at 37°C and then examined by reducing SDS-PAGE, Western blotting and detection with chemiluminescence. *B,* The FRET signal, determined as described in *Materials and Methods*, seen after the indicated constructs were transfected into 293T cells, was determined 48 h after transfection. The signal is measured following incubation of the cells at 4°C, room temperature (~23°C), or 37°C, respectively.

Since CD23 interacts in a divalent manner with IgE, binding avidity is brought into play, potentially canceling the differences in affinity measurements found between IgE and FcεRI compared with CD23 vs IgE (10^9–10^{11} M^{-1} vs 10^7–10^8 M^{-1}, respectively) (34, 35). The above studies demonstrated >90% inhibition of binding with a 10-fold molar excess of *lz*-CD23, suggesting its potential as an alternative to the currently used anti-IgE. These initial studies were all performed at 4°C, a standard binding assay temperature. When the binding studies were extended to determine whether mediator release was also inhibited using 37°C sensitization, minimal inhibition of mediator release was seen even up to a 1000-fold excess of *lz*-CD23. This result was explained when binding assays were performed at different temperatures. The effectiveness of *lz*-CD23 as an inhibitor of IgE binding decreased as temperatures approached 37°C. Although 40–50% inhibition of binding continued to occur at 37°C, the lack of mediator release

inhibition is presumably explained in that sufficient IgE is still bound for an efficient cross-linking signal to be given.

The next obvious question is what is causing the change with temperature—a change in the receptors or a change in IgE. The first consideration examined was a change in CD23. Clearly, if dissociation of *lz*-CD23 occurs, then the monomeric *lz*-CD23 would not be expected to influence FcεRI-IgE interaction. Both chemical cross-linking and FRET studies (Fig. 7) indicate that the *lz*-CD23 is not undergoing significant dissociation at 37°C. Indeed, the FRET analyses show an increased signal for the *lz*-CD23 as compared with membrane CD23. Although the reasons for this increased FRET signal are unknown, the attachment of the CFP/YFP donor acceptor directly to the *lz* motif may enhance the FRET signal. In separate studies to be reported elsewhere, we have characterized an anti-stalk mAb that binds more effectively to CD23 at elevated temperatures (1:1 at 4°C vs 3:1 at 37°C for binding of mAb to CD23, respectively). These studies indicate that membrane CD23 is a less stable oligomer at 37°C, although clearly, complete dissociation is not seen.

When SPR analysis was performed at different temperatures, evidence for a change in IgE was observed. CD23 has long been known to interact with IgE with a dual affinity (5); the conditions used for SPR do not detect the low-affinity interaction, as evidenced by the lack of signal for the mouse and human sCD23 extracellular domain (14). With respect to high-affinity interaction, SPR indicates that less of the IgE bound to the chip is available for interaction with CD23 at higher temperatures. This is seen in the binding sensorgrams shown in Fig. 3 for different concentrations of mouse *lz*-CD23 analyzed at 15 and 35°C. Although the binding parameters (Table I) did not show significant changes, the plateau binding was significantly decreased at all *lz*-CD23 concentrations examined. This drop vs temperature is further illustrated by Fig. 4, where the plateau binding value is shown as a function of temperature for a single human or mouse *lz*-CD23 concentration. A reversible drop in available IgE is seen.

Analysis of binding to cell surface CD23 or FcεRI further substantiates the differences seen in that binding to CD23 is more effective at 4°C whereas the converse is true for the FcεRI, namely, binding is more effective with increasing temperatures. The cell surface binding studies also allowed us to examine both low- and high-affinity binding for CD23 at different temperatures and, as seen in Fig. 5B, the most drastic changes occur in the high-affinity binding parameter, going from 5.6×10^7 M^{-1} (4°C) to 1.5×10^7 M^{-1} (37°C). The low affinity also changes somewhat, but this may be due to a decreased influence from the high-affinity component. Fig. 5A represents a determination of the amount of bindable IgE in the preparation and, based on the SPR analyses, we anticipated that less bindable IgE would be seen at the elevated temperature. Indeed, this was exactly what was seen. Analysis of IgE binding to the FcεRI was also informative in that the bindability now was increased at 37°C as compared with 4°C, exactly the opposite of what is seen with CD23. In contrast to CD23, however, a similar amount of IgE was bound at both temperatures, albeit more slowly at the lower temperature (Fig. 6B).

A potential explanation for this data is seen in the reported crystal structure of IgE Fc and IgE-Fc-FcεRI complexes (16). IgE Fc was found to be in what was termed an open and closed configuration while the open configuration was exclusively found when complexed to the FcεRI (13). These authors proposed that the two isoforms of IgE might interact with the two receptors differently. Although definitive proof of this hypothesis awaits analysis of CD23-IgE-Fc complexes, the data in this study would fit this concept, namely, that the closed configuration would be anticipated to predominate at lower temperatures and interact more effectively

with CD23, whereas the open configuration is seen at 37°C with more effective interaction with the FcεRI. The data would also suggest that the closed configuration interacts less effectively (if at all) with the FcεRI. The slower interaction seen at 4°C could potentially be the result of converting to the open configuration. Thus, a strategy to prevent binding to the FcεRI would be to prevent the conversion to the open configuration. This could potentially be done with appropriate anti-IgE mAbs or with CD23. In the latter case, the increased instability of the oligomer at the elevated temperatures precludes its use. We are currently attempting to increase the stability of this oligomer by increasing the stability of the coiled-coil stalk region.

The decreased capacity of CD23 to interact with IgE at physiological temperature combined with studies indicating that CD23 can regulate IgE production (9, 36) appear contradictory. One potential explanation is that the interaction with alternate ligands such as CD21 (37), CD11 (38), or CD47-vitronectin (39) is both not temperature sensitive and is triggering the observed IgE regulation. Alternatively, the multipoint interaction when both the CD23 and surface IgE are membrane bound may make a lower affinity interaction sufficient for triggering. More work will be required to understand the mechanisms involved.

Acknowledgments

References

1. Nadler, M. J., S. A. Matthews, H. Turner, and J. P. Kinet. 2000. Signal transduction by the high-affinity immunoglobulin E receptor FcεRI: coupling form to function. *Adv. Immunol. 76:325.*

2. Blank, U., C. Ra, L. Miller, K. White, H. Metzger, and J.-P. Kinet. 1989. Complete structure and expression in transfected cells of high affinity IgE receptor. *Nature 337:187.*

3. Ra, C., M.-H. Jouvain, and J.-P. Kinet. 1989. Complete structure of the mouse mast cell receptor for IgE (FcεRI) and surface expression of chimeric receptors (rat-mouse-human) on transfected cells. *J. Biol. Chem. 264:15323.*

4. Conrad, D. H. 1998. Structure and function of CD23. In *The Immunoglobulin Receptors and their Physiological and Pathological Roles in Immunity*, Vol. 26. J. G. J. Van de Winkel and P. M. Hogarth, eds. Kluwer, Boston, p. 195.

5. Dierks, S. E., W. C. Bartlett, R. L. Edmeades, H. J. Gould, M. Rao, and D. H. Conrad. 1993. The oligomeric nature of the murine FcεRII/CD23: implications for function. *J. Immunol. 150:2372.*

6. Gould, H., B. Sutton, R. Edmeades, and A. Beavil. 1991. CD23/FcεRII: C-type lectin membrane protein with a split personality. *Monogr. Allergy 29:28.*

7. Marolewski, A. E., D. R. Buckle, G. Christie, D. L. Earnshaw, P. L. Flamberg, L. A. Marshall, D. G. Smith, and R. J. Mayer. 1998. CD23 (FcεRII) release from cell membranes is mediated by a membrane-bound metalloprotease. *Biochem. J. 333:573.*

8. Kehry, M. R., and L. C. Yamashita. 1989. Fcε receptor II (CD23) function on mouse B cells: role in IgE dependent antigen focusing. *Proc. Natl. Acad. Sci. USA 86:7556.*

9. Payet-Jamroz, M., S. L. Helm, J. Wu, M. Kilmon, M. Fakher, A. Basalp, J. G. Tew, A. K. Szakal, N. Noben-Trauth, and D. H. Conrad. 2001. Suppression of IgE responses in CD23-transgenic animals is due to expression of CD23 on nonlymphoid cells. *J. Immunol. 166:4863.*

10. Yu, P., M. Kosco-Vilbois, M. Richards, G. Köhler, M. C. Lamers, and G. Kohler. 1994. Negative feedback regulation of IgE synthesis by murine CD23. *Nature 369:753.*

11. Keegan, A. D., C. Fratazzi, B. Shopes, B. Baird, and D. H. Conrad. 1991. Characterization of new rat anti-mouse IgE monoclonals and their use along with chimeric IgE to further define the site that interacts with FcεRII and FcεRI. *Mol. Immunol. 28:1149.*

12. Vercelli, D., B. Helm, P. Marsh, E. Padlan, R. S. Geha, and H. Gould. 1989. The B-cell binding site on human immunoglobulin E. *Nature 338:649.*

13. Garman, S. C., B. A. Wurzburg, S. S. Tarchevskaya, J. P. Kinet, and T. S. Jardetzky. 2000. Structure of the Fc fragment of human IgE bound to its high-affinity receptor FcεRIα. *Nature 406:259.*

14. Chen, B.-H., C. Ma, T. H. Caven, Y. Chan-Li, A. Beavil, B. Beavil, H. Gould, and D. H. Conrad. 2002. Necessity of the stalk region for IgE interaction with CD23. *Immunology. 107:373.*

15. Kelly, A. E., B.-H. Chen, E. C. Woodward, and D. H. Conrad. 1998. Production of a chimeric form of CD23 that is oligomeric and blocks IgE binding to the FcεRI. *J. Immunol. 161:6696.*

16. Wurzburg, B. A., S. C. Garman, and T. S. Jardetzky. 2000. Structure of the human IgE-Fc Cε3-Cε4 reveals conformational flexibility in the antibody effector domains. *Immunity 13:375.*

17. Wiegand, T. W., P. B. Williams, S. C. Dreskin, M.-H. Jouvain, J. P. Kinet, and D. Tasset. 1996. High-affinity oligonucleotide ligands to human IgE inhibit binding to Fcε receptor I. *J. Immunol. 157:221.*

18. Bazin, H., and A. Beckers. 1976. IgE myelomas in rats. In *Molecular and Biological Aspects of the Acute Allergic Reaction*. S. G. O. Johansson, K. Strandberg, and B. Uvnas, eds. Plenum, New York, p. 125.

19. Liu, F. T., J. W. Bohn, E. L. Ferry, H. Yamamoto, C. A. Molinaro, L. A. Sherman, N. R. Klinman, and D. H. Katz. 1980. Monoclonal dinitrophenyl-specific murine IgE antibody: preparation, isolation, and characterization. *J. Immunol. 124:2728.*

20. Isersky, C., A. Kulczycki, Jr., and H. Metzger. 1974. Isolation of IgE from reaginic rat serum. *J. Immunol. 112:1909.*

21. Young, R. J., R. J. Owens, G. A. Mackay, C. M. Chan, J. Shi, M. Hide, D. M. Francis, A. J. Henry, B. J. Sutton, and H. J. Gould. 1995. Secretion of recombinant human IgE-Fc by mammalian cells and biological activity of glycosylation site mutants. *Protein Eng. 8:193.*

22. McConahey, P. J., and F. J. Dixon. 1966. A method for trace iodination of proteins for immunologic studies. *Int. Arch. Allergy Appl. Immunol. 29:185.*

23. McDonnell, J. M., A. J. Beavil, G. A. Mackay, B. A. Jameson, R. Korngold, H. J. Gould, and B. J. Sutton. 1996. Structure based design and characterization of peptides that inhibit IgE binding to its high-affinity receptor. *Nat. Struct. Biol. 3:419.*

24. Conrad, D. H., A. D. Keegan, K. R. Kalli, R. Van-Dusen, M. Rao, and A. D. Levine. 1988. Superinduction of low affinity IgE receptors on murine B lymphocytes by lipolysaccharide and IL-4. *J. Immunol. 141:1091.*

25. Lindmo, T., E. Boven, F. Cuttitta, J. Fedorko, and P. A. Bunn, Jr. 1984. Determination of the immunoreactive fraction of radiolabeled monoclonal antibodies by linear extrapolation to binding at infinite antigen excess. *J. Immunol. Methods 72:77.*

26. Dower, S. K., C. DeLisi, J. A. Titus, and D. M. Segal. 1981. Mechanism of binding of multivalent immune complexes to Fc receptors. 1. Equilibrium binding. *Biochemistry 20:6326.*

27. Cook, J. P., A. J. Henry, J. M. McDonnell, R. J. Owens, B. J. Sutton, and H. J. Gould. 1997. Identification of contact residues in the IgE binding site of human FcεRIα. *Biochemistry 36:15579.*

28. Siegel, R. M., J. K. Frederiksen, D. A. Zacharias, F. K. Chan, M. Johnson, D. Lynch, R. Y. Tsien, and M. J. Lenardo. 2000. Fas preassociation required for apoptosis signaling and dominant inhibition by pathogenic mutations. *Science 288:2354.*

29. Gordon, G. W., G. Berry, X. H. Liang, B. Levine, and B. Herman. 1998. Quantitative fluorescence resonance energy transfer measurements using fluorescence microscopy. *Biophys. J. 74:2702.*

30. Jiang, X., and A. Sorkin. 2002. Coordinated traffic of Grb2 and Ras during epidermal growth factor receptor endocytosis visualized in living cells. *Mol. Biol. Cell 13:1522.*

31. Shi, J., R. Ghirlando, R. L. Beavil, A. J. Beavil, M. B. Keown, R. J. Young, R. J. Owens, B. J. Sutton, and H. J. Gould. 1997. Interaction of the low-affinity receptor CD23/FcεRII lectin domain with the Fcε3–4 fragment of human immunoglobulin E. *Biochem. 36:2112.*

32. Bartlett, W. C., A. E. Kelly, C. M. Johnson, and D. H. Conrad. 1995. Analysis of murine soluble FcεRII sites of cleavage and requirements for dual-affinity interaction with IgE. *J. Immunol. 154:4240.*

33. Beavil, A. J., R. L. Edmeades, H. J. Gould, and B. J. Sutton. 1992. α-Helical coiled-coil stalks in the low-affinity receptor for IgE (FcεRII/CD23) and related C-type lectins. *Proc. Natl. Acad. Sci. USA 89:753.*

34. Rossi, G., S. A. Newman, and H. Metzger. 1977. Assay and partial characterization of the solubilized cell surface receptor for immunoglobulin E. *J. Biol. Chem. 252:704.*

35. Lee, W. T., and D. H. Conrad. 1986. Murine B cell hybridomas bearing ligand-inducible Fc receptors for IgE. *J. Immunol. 136:4573.*

36. Nakamura, T., W. S. Kloetzer, P. Brams, K. Hariharan, S. Chamat, X. Cao, M. J. LaBarre, P. C. Chinn, R. A. Morena, W. S. Shestowsky, et al. 2000. In vitro IgE inhibition in B cells by anti-CD23 monoclonal antibodies is functionally dependent on the immunoglobulin Fc domain. *Int. J. Immunopharmacol. 22:131.*

37. Aubry, J. P., S. Pochon, P. Graber, K. U. Jansen, and J.-Y. Bonnefoy. 1992. CD21 is a ligand for CD23 and regulates IgE production. *Nature 358:505.*

38. Pochon, S., P. Graber, M. Yeager, K. Jansen, A. R. Bernard, J.-P. Aubry, and J.-Y. Bonnefoy. 1992. Demonstration of a second ligand for the low affinity receptor for immunoglobulin E (CD23) using recombinant CD23 reconstituted into fluorescent liposomes. *J. Exp. Med. 176:389.*

39. Hermann, P., M. Armant, E. Brown, M. Rubio, H. Ishihara, D. Ulrich, R. G. Caspary, F. P. Lindberg, R. Armitage, C. Maliszewski, et al. 1999. The vitronectin receptor and its associated CD47 molecule mediates proinflammatory cytokine synthesis in human monocytes by interaction with soluble CD23. *J. Cell Biol. 144:767.*